MicroRNAs regulate critical genes associated with multiple myeloma pathogenesis

Flavia Pichiorri*†, Sung-Suk Suh*†, Marco Ladetto‡, Michael Kuehl§, Tiziana Palumbo*, Daniela Drandi‡, Cristian Taccioli*, Nicola Zanesi*, Hansjuerg Alder*, John P. Hagan*, Reinhold Munker¶, Stefano Volinia*, Mario Boccadoro‡, Ramiro Garzon‖, Antonio Palumbo‡, Rami I. Aqeilan*,**, and Carlo M. Croce*,††

Departments of *Molecular Virology, Immunology, and Human Genetics, and ‖Division of Hematology and Oncology, Department of Medicine, Comprehensive Cancer Center, Ohio State University, Columbus, OH 43210; ‡Division of Hematology, University of Torino, 10126 Torino, Italy; §Genetics Branch, Center for Cancer Research, National Cancer Institute, Bethesda, MD 20889-5105; and ¶Division of Hematology/Oncology, Louisian State University Health Sciences Center, Louisiana State University, Shreveport, LA 71130

Contributed by Carlo M. Croce, June 27, 2008 (sent for review June 1, 2008)

Progress in understanding the biology of multiple myeloma (MM), a plasma cell malignancy, has been slow. The discovery of microRNAs (miRNAs), a class of small noncoding RNAs targeting multiple mRNAs, has revealed a new level of gene expression regulation. To determine whether miRNAs play a role in the malignant transformation of plasma cells (PCs), we have used both miRNA microarrays and quantitative real time PCR to profile miRNA expression in MM-derived cell lines ($n = 49$) and CD138+ bone marrow PCs from subjects with MM ($n = 16$), monoclonal gammopathy of undetermined significance (MGUS) ($n = 6$), and normal donors ($n = 6$). We identified overexpression of *miR-21*, *miR-106b*~*25* cluster, *miR-181a* and *b* in MM and MGUS samples with respect to healthy PCs. Selective up-regulation of *miR-32* and *miR-17*~*92* cluster was identified in MM subjects and cell lines but not in MGUS subjects or healthy PCs. Furthermore, two miRNAs, *miR-19a* and *19b*, that are part of the *miR-17*~*92* cluster, were shown to down regulate expression of SOCS-1, a gene frequently silenced in MM that plays a critical role as inhibitor of IL-6 growth signaling. We also identified p300-CBP-associated factor , a gene involved in p53 regulation, as a bona fide target of *the miR106b*~*25* cluster, *miR-181a* and *b*, and *miR-32*. Xenograft studies using human MM cell lines treated with *miR-19a* and *b*, and *miR-181a* and *b* antagonists resulted in significant suppression of tumor growth in nude mice. In summary, we have described a MM miRNA signature, which includes miRNAs that modulate the expression of proteins critical to myeloma pathogenesis.

PCAF | SOCS-1 | tumor suppressor gene | MGUS | plasma cells

Multiple myeloma (MM) is a B-cell neoplasm characterized by the accumulation of clonal malignant plasma cells in the bone marrow (1). This cancer can occur *de novo* or develop from a benign condition called monoclonal gammopathy of undetermined significance (MGUS) at a rate of ≈1% per year (2–3). MM cells are endowed with a multiplicity of antiapoptotic signaling mechanisms, which account for resistance to current chemotherapy regimens (4). Therapeutic modalities that are effective in MM modulate levels of the proapoptotic and antiapoptotic Bcl-2 family of proteins and of inhibitors of apoptosis, which are primarily regulated by p53 (mutated at low frequency in MM) (4). It is well known that the bone marrow microenvironment plays a prominent role in the biology of MM; adhesion of MM cells to the bone marrow stroma triggers cytokine production, enhances cell proliferation and resistance to chemotherapy by activation of NFκB, phosphatidyl-inositol 3-kinase PIK/AKT and signal transducer and activator of transcription 3 (STAT-3) pathways through the best characterized MM growth factor, IL-6 (3, 4).

Detailed genomic analysis has revealed that MM has complex cytogenetic abnormalities (4–6). For example, aneuploidy, assessed by interphase fluorescence *in situ* hybridization and DNA flow cytometry (6), is observed in >90% of cases (5–6). In addition to chromosome number aberrations, specific cytogenetic abnormalities in MM are typically complex, including reciprocal chromosomal translocations involving the Ig H locus [eg, t (4, 14), t (6, 14), t (14, 16)], chromosome 13 monosomy, loss of the short arm of chromosome 17, and gains or amplifications of the long arm of the chromosome 1 (3). The presence of RAS family member mutations at codons 12, 13, and 61 of *NRAS* and *KRAS*, has been described in ≈30 to 35% of MM patients and 45% of MM cell lines (7), and more importantly it seems that is the major genetic difference between MM and MGUS (3–7).

Despite recent advances in oncogenomics and MM cell-stroma interactions, further studies are needed to identify critical players in MM pathogenesis that could be targeted by pharmacological intervention to improve outcomes for this still incurable disease. The advent of new techniques, such as microarray gene expression, including noncoding RNAs, may lead to an improved understanding of MM biology by establishing associations between gene expression changes and MM molecular and clinical features, as shown by us for chronic lymphoid and acute myelogenous leukemia (8–9).

MicroRNAs (miRNAs) are noncoding RNAs of 19 to 25 nucleotides in length that regulate gene expression by inducing translational inhibition and degradation of their target mRNAs through base pairing to partially or fully complementary sites (10). MiRNAs are involved in critical biological processes, including development, cell differentiation, stress response, apoptosis, and proliferation (10). Recently, specific miRNA expression patterns have been linked to hematopoiesis and cancer (11–13). Little is known, however, about miRNA expression in MM. A recent study has shown that, in IL-6 dependent MM cell lines, *miR-21* transcription is controlled by IL-6 through a STAT-3 mechanism. Moreover, ectopic *miR-21* expression is sufficient to sustain growth of IL-6-dependent cell lines in the

CELL BIOLOGY

Author contributions: F.P., S.-S.S., M.K., T.P., D.D., C.T., N.Z., S.V., M.B., A.P., R.I.A., and C.M.C. designed research; F.P., S.-S.S., M.L., M.K., T.P., D.D., C.T., N.Z., H.A., J.P.H., R.M., S.V., and R.I.A. performed research; F.P., S.-S.S., M.L., M.K., T.P., D.D., C.T., H.A., J.P.H., R.M., S.V., M.B., R.G., A.P., R.I.A., and C.M.C. contributed new reagents/analytic tools; F.P., S.-S.S., M.K., C.T., H.A., S.V., R.G., A.P., R.I.A., and C.M.C. analyzed data; and F.P., R.G., and R.I.A. wrote the paper.

The authors declare no conflict of interest.

Data deposition: The microarray data have been deposited in the Array Express database, www.ebi.ac.uk/arrayexpress (accession no. E-TABM-508).

†F.P. and S.S. contributed equally to this work.

**To whom correspondence may be addressed at: Molecular Virology, The Lautenberg Center for General and Tumor Immunology, Hebrew University of Jerusalem, Jerusalem 91120, Israel. E-mail: aqeilan@cc.huji.ac.il.

††To whom correspondence may be addressed at: Ohio State University Comprehensive Cancer Center, Wiseman Hall Rm 385L, 410 West 12th Avenue, Columbus, OH 43210. E-mail: carlo.croce@osumc.edu

This article contains supporting information online at www.pnas.org/cgi/content/full/0806202105/DCSupplemental.

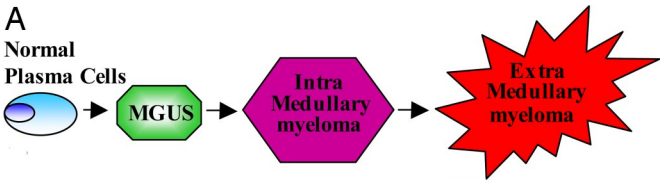

B

miRNA	Fold change MGUS
miR-21	15.6
miR-181a	13.9
* *miR-93*	13.4
* *miR-106b*	10.4
* *miR-25*	7.04
** *miR-106a*	5.84
miR-328	0.15

C

miRNA	Fold change Patients	Fold change MM PCs
* *miR-25*	71.4	224.3
miR-32	51.4	288.9
** *miR-20a*	18.1	72.0
* *miR-93*	14.8	48.2
** *miR-106b*	11.8	38.5
* *miR-106a*	11.2	67.1
miR-181a	9.3	25.5
miR-21	9.1	24.1
** *miR-19a*	ND	33.7
** *miR-19b*	5.9	7.1
miR-181b	5.4	13.7
** *miR-92a*	4.6	11.6
miR-328	0.49	0.47

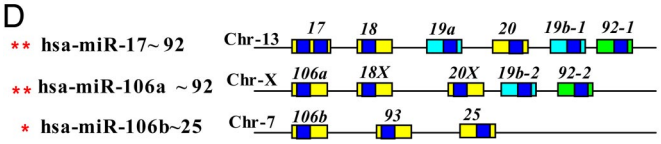

Fig. 1. MM and MGUS express a distinct spectrum of miRNA in comparison to normal CD138+ PCs. (*A*) Schematic drawing showing the multistep molecular process of PC transformation. (*B*) Representative list of the miRNAs significantly deregulated in MGUS versus normal PCs analyzed in this study. The asterisks indicate the specific associated cluster. (*C*) Representative list of the common deregulated miRNAs in the comparison classes MM patient versus normal PCs and PCs MM versus normal PCs analyzed in this study. The asterisks indicate the specific associated cluster. (*D*) *miR-17* microRNA clusters. Three paralog families of miRNA precursors can be identified: *miR-17/18/18X/20/93/106a/106b/93* (*yellow*), *mir-19a/19b-1/19b-2* (*blue*) and *mir-92-1/92-2/25* (*green*).

absence of IL-6 (14). Here, we have used both miRNA microarrays and quantitative RT-PCR to assess the miRNA expression in MM-derived cell lines and CD138+ bone marrow plasma cells (PCs) from MM subjects, MGUS, and normal donors. Our findings define an miRNA signature related to expression and regulation of proteins associated with malignant transformation of PCs.

Results

A Characteristic miRNA Signature Differentiates MGUS from Healthy PCs. Current models assume that MM evolves through a multistep transformation process (Fig. 1*A*) (15). To identify specific alterations associated with early pathogenetic events of MM, we profiled five CD138+ PCs from MGUS subjects and four healthy PCs [see supporting information (SI) Table S1 for patient characteristics] by using our miRNA microarray platform. We first compared MGUS to the healthy counterpart PCs by using the univariate *t* test within BRB tools (class comparison) (Fig. 1*B* and Table S2). We found 48 miRNAs significantly deregulated ($P \leq 0.05$); 41 miRNAs were up-regulated and 7 down-regulated in MGUS with respect to normal CD138+ PCs (see Table S2, a representative list is shown in Fig. 1*B*). The most up-regulated miRNAs in MGUS were *miR-21*, which was described by other groups to be up-regulated in MM as well (14), *miR-181a*, known to have a role in B and T cell differentiation (16), and the oncogenic cluster *miR-106b~25*, in particular *miR-93*, *miR-106b*, and *miR-25* (see Fig. 1*B* and Table S2).

MiRNA Signatures in MM Patients and Cell Lines. To determine whether miRNAs are deregulated in MM, we analyzed the global miRNA expression in 41 MM-derived cell lines (Table S3), CD138+ untreated bone marrow PCs from 10 MM, and 4 normal CD138+ PCs using our miRNA microarray (17). The degree of CD138+PCs purity after AutoMACs automated separation system (Miltenyi-Biotec) and the clinical features of the MM cases and normal PCs are listed in Table S1. First, we compared miRNA expression in primary tumors and cell lines compared to CD138+ healthy controls using univariate *t* test within by BRB (Table S4). Our analysis revealed up-regulation of 60 and down-regulation of 36 miRNAs in MM subjects and cell lines compared to CD138+ healthy controls (see Fig. 1*C* and Table S4). All miRNAs have a fold-change >2 and a P value ≤ 0.01. Because miRNA expression in cell lines could be also deregulated because of prolonged *in vitro* culture, we analyzed the miRNA expression only in MM subjects versus healthy PCs (Table S5). We found 37 up- and 37 down-regulated miRNAs in MM subjects with respect to normal PCs with a fold-change >2 and a P value ≤ 0.01 (see Table S5). Approximately 90% of the up-regulated miRNAs (34 out of 37) and 30% of the down-regulated miRNAs (10 out of 37) were in common to the combined group of MM subjects and cell lines, thereby validating our approach of combining cell lines and MM subject samples, at least for the analysis of up-regulated miRNAs (see Fig. 1*C* and Table S6). A Venn diagram in Fig. S1 shows the common miRNAs between these two groups of comparison. Similar to the signature observed in MGUS, *miR-21* and the *miR-106a~92* cluster were found up-regulated in MM subjects and cell lines (see Fig. 1*C* and Table S3). However, we identified that *miR-32* and the cluster *miR-17~92* (in particular *miR-19a* and *b*) were significantly up-regulated only in MM samples but not in MGUS or healthy PCs (see Fig. 1*C*), indicating a possible role in the malignant transformation from MGUS to MM.

Validation of the miRNA Signatures by q-RT-PCR. To validate the microarray results we performed quantitative real time PCR (q-RT-PCR) for *miR-32*, *miR-17–5*, *miR-19a*, *miR-19b*, *miR-20a*, *miR-92*, *miR-106a (miR-17~92* cluster), *miR-106b*, *miR-93* and *miR-25 (miR-106b~25* cluster), *miR-328*, and *miR-181a* and *b* using an independent set of randomly chosen CD138+PCs from healthy subjects ($n = 3$), MM patient samples ($n = 6$), and MGUS ($n = 3$) (see Table S1), all from different donors, plus a set of MM cell lines ($n = 15$) (see Table S1). We confirmed the over-expression of the *miR-106b~25* cluster in MGUS and MM samples with respect to the CD138+ healthy PCs (Fig. S2*A*). Although the *miR-106b~25* cluster shares a high degree of homology with the *miR-17~92* cluster (Fig. 1*D*), and an oncogenic role was reported for both (18–20), we are confident of the specificity of stem-loop q-RT-PCR for the analysis of highly similar miRNAs; a previous report from our laboratory showed exquisite specificity of *miR-106b*, *miR-93*, and *miR-25* primers (20). Mature *miR-181a* was over-expressed in 2 out of 3 MGUS, 6 out of 6 MMs, and 9 out of 15 cell lines with an average on the differential expression shown in Fig. S2*B*. In addition, *miR-181b* was also over-expressed in MM and MGUS, albeit at a lower degree than *miR-181a* (see Fig. S2*B*). We further validated the over-expression of the *miR-32* and *miR-17~92* cluster (Fig. S2 *C–F*) in MM patients and cell lines. Consistent with the array data, the two *miR-17~92* cluster members, *miR-19a* and *b* and *miR-32*, were highly over-expressed in 6 out of 6 MM PC samples and 15 out of 15 cell lines (see Fig. S2 *C* and *F*). Principally, we found that *miR-19a* and *b* have a fold-change >100 times (see Fig. S2*F*), although they show very low expression in 1 out of 3

MGUS and almost no expression in 2 out of 3 MGUS and 3 out of 3 healthy PC samples, validating our initial array results and suggesting that these miRNAs are MM-specific.

Several miRNAs Up-Regulated in MM Target p300-CBP-Associated Factor , a Positive Regulator of p53. One of the most up-regulated miRNAs in MGUS and MM patients and cell lines were *miR-181a* and *b*, and *miR-106b~25*, while *miR-32* was preferentially up-regulated in MM. Using "in silico" target prediction software [Target Scan (21), Pictar (22)], we found that those miRNAs are predicted to target the 3′-UTR of the p300-CBP-associated factor (PCAF) (Fig. 2*A*). PCAF is a histone acetyltransferase involved in the reversible acetylation of various transcriptional regulators, including the tumor suppressor protein p53 (23). Recently, Linares and colleagues have shown that PCAF possesses an intrinsic ubiquitination activity that is critical for controlling Hdm2 expression levels, and thus p53 (24) that is rarely mutated (5–10% of cases) or deleted at diagnosis in MM (25–26). To examine whether these miRNAs could regulate PCAF, first we analyzed PCAF expression by q-RT-PCR (Fig. S3*A*) and Western blotting (Fig. S3*B*) in 15 MM cell lines. As control, we used two CD138+PCs isolated from healthy donors. We found that PCAF expression is almost absent (10-fold less than in control) in 10 out of 15 cell lines, whereas the remaining 5 cell lines displayed very low expression. To investigate whether this gene was deleted at the genomic level we performed whole genome comparative genomic hybridization analysis of all 15 MM cell lines using the Affymetrix SNP 6.0 arrays. However, we did not observe deletion of the *PCAF* gene (data not shown). Second, we cloned the *PCAF* 3′ UTR into a luciferase reporter vector and cotransfected with the candidate miRNAs mimics or scrambled oligonucleotides and performed luciferase assays as described in *Methods*. We found that *miR-181a* and *b* (Fig. 2*B*), *106b~25* cluster and *32* (Fig. 2 *D* and *B)*, interact with the *PCAF* 3′UTR *in vitro*. However, this interaction was less significant with *miR-92* (Fig. 2*C*) and no interaction was observed with *miR-19a* and *b* (data not shown). Mutation of the predicted miRNA binding sites in the reporter vector abrogated this effect, indicating that these miRNAs directly interact with the *PCAF* 3′UTR. To confirm the biological role of these miRNAs in *PCAF* regulation in MM cells, we validated the *in vitro* studies by antagonizing endogenous *miR-181a*, *181b*, *25*, *93*, *106b* and *92* using antisense oligos (ASOs) in U266 and JJN3 MM cell lines. In both cell lines the antagomiRs induced accumulation of PCAF protein expression at 72 h after transfection (Fig. 2 *E* and *F*). By contrast over-expression of the same miRNAs by oligonucleotide transfection reduced PCAF expression in the K562 cell line (Fig. 2 *G* and *H*). *MiR-19a* and *b* did not influence PCAF expression (Fig. 2*H*) and *miR-92* had little effect on its expression (see Fig. 2*F*), confirming the luciferase expression data (see Fig. 2*C*). To determine whether the miRNA regulators of PCAF are able to indirectly affect p53 expression, we transfected MM1 cells with anti-*miR-181a* and *b* or with all antagomiRs simultaneously (anti-*miRs-181s*, *93*, *106b*, *25*, *32*) exposed the cells to UV (UV) radiation (Fig. 2*I*) and measured the expression of p53 and PCAF by q-RT-PCR (see Fig. 2*I*). Fig. S4*A* shows the re-expression of PCAF protein after 48 h of antagomiRs treatment. The antagonizing activity of transfectant oligos is shown in Fig. S4*B*. After UV treatment, p53 mRNA expression was almost doubled in cells transfected with antisense *miR-181a* and *b*, while it increased sixfold after nucleoporation with all antagomiRs simultaneously (see Fig. 2*I*). Furthermore, after transfection of antisense *miR-181a* and *b* oligos in MM1s, we treated the cells with a small-molecule MDM2 antagonist nutlin-3a (10 μM) and measured p53 by Western blotting. We found that the cells transfected with *miR-181* ASOs displayed a higher level of p53 protein compared to scrambled and *miR-92* ASOs at 9 and 12 h (Fig. 2*L*). Together, these data show that the *miR-106b-25*

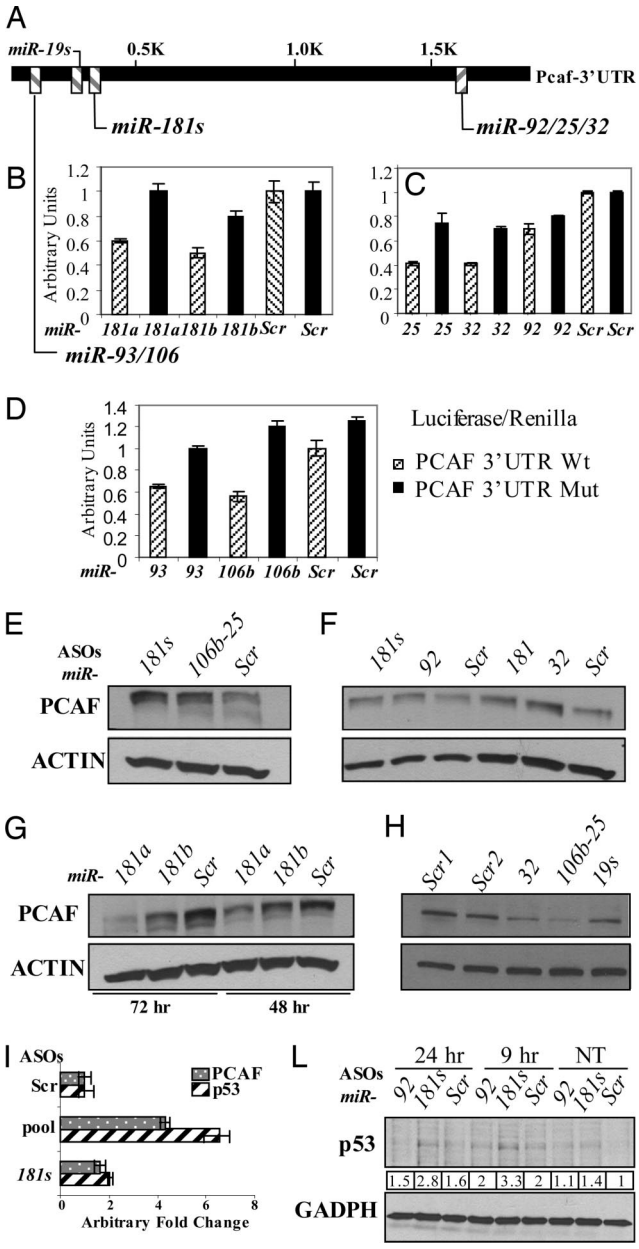

Fig. 2. *miR-181s*, *106b-25 cluster*, *32* target PCAF. (*A*) miRNAs predicted to interact with *PCAF* gene in several consensus binding sites at its 3′-UTR, according to "in silico" target Target Scan prediction software. (*B–D*) Luciferase assay showing decreased luciferase activity in cells cotransfected with *pGL3-PCAF-3′UTR* and *miR-181s* (*B*), *miR-32/miR-25/miR-92* (*C*), and *miR-93/miR-106b* (*D*) oligonucleotides. Deletion of six bases in three putative *miR-181s*, *miR-106b/miR-93*, and *miR-32/miR-25/miR-92* binding sites, complementary to miRNAs seed regions, abrogates this effect (MUT). Bars indicate firefly luciferase activity normalized to Renilla luciferase activity ± SD. Each reporter plasmid was transfected at least twice (on different days) and each sample was assayed in triplicate. (*E*, *F*) Immunoblot analyses showing PCAF and GADPH expression after transfection with *miR-181s* and *miR-106b/25 cluster* ASOs in U266 cells (*E*) and with *miR-181s*, *miR-32 and miR-92* ASOs in JJN3 cells (*F*), or mimics in K562 cells (*G*, *H*). (*I*) Real-time RT-PCR analyses for p53 and PCAF expression in MM1s cells transfected with *miR-181a* and *b* or with *miR-181a* and *b* and *miR-106b/25* together ASOs (pool) or with scrambled oligonucleotide at 48 h after transfection and after 4 h of UV treatment. The PCR products for both genes were normalized to GADPH and ACTIN expression. The bar-graph represents the mean values observed in four separate studies ± SE. (*L*) Immununoblot analysis showing p53 protein expression after 48 h of *miR-181a*, *miR-181b*, *miR-92* and scrambled ASOs transfection in MM1 cells after 9 h and overnight incubation with 10 μM nutlin-3a; GADPH was internal loading control. Densitometry based on GADPH levels shows increased level of p53 in presence of *miR-181a* and *miR-181b* ASOs in MM1s cells.

CELL BIOLOGY

cluster, *miR-32*, *miR-181a* and *b* target PCAF and through this gene, indirectly control p53 activity in myeloma.

***miR-19a* and *miR-19b* Target SOCS-1, a Negative Regulator of IL-6R/STAT-3 Pathway.** Our findings indicate that *miR-19a* and *b* are up-regulated >100-fold in patient samples, >2,000 times in the cell lines (Fig. S2*F*), and are both almost absent in normal PCs and MGUS. These data suggest that both miRNAs contribute to the development of MM. Therefore, we searched for *miR-19a* and *b* mRNA targets, which are involved in myeloma pathogenesis, using available target-prediction software [Target Scan (21), Pictar (22)]. Among >100 predicted targets, SOCS-1 has been implicated in the negative regulation of several cytokine pathways including IL-6, particularly the Jak/STAT pathways (27), and is frequently silenced by methylation in MM (28). We therefore hypothesized that the high levels of *miR-19s* levels in MM samples may play an important role in the constitutive activation of Jak/STAT-3 signaling through down-regulation of its negative regulator SOCS-1. To examine our hypothesis, we first assessed its expression in 15 MM cell lines and two healthy CD138+ PCs and found almost no protein expression in 13 out of 15 cell lines compared to control (Fig. 3*A*). To examine whether SOCS-1 reduced expression levels could be a consequences of up-regulated *miR-19a* and *b* in MM cells, we performed Western blot analysis using SOCS-1 antibody after transfection of candidate antagomiRNAs or scrambled oligonucleotides in U266 (which has an active IL-6 autocrine loop) (29) and JJN3 MM cell lines that display reduced SOCS-1 expression (Fig. 3*D*). Moreover, *miR-19a* and *miR-19b* mimics inhibited the expression of a reporter vector containing SOCS-1 3′UTR, while mutation of the predicted miRNA-binding site abrogated this effect (Fig. 3 *B* and *C*). As shown in Fig. 3 *C* and *D*, there was significant up-regulation of SOCS-1 protein in U266 and JJN3 cells transfected with antisense oligonucleotide for *miR-19a* and *b* but not with scrambled oligonucleotides. Furthermore, constitutive STAT-3 phosphorylation in U266 cells was markedly decreased at 72 h after transfection by anti-*miR-19s* but not by scrambled (Fig. 3*E*). The ASOs activity at 72 h was detected by q-RT-PCR (Fig. 3*F*). These studies suggest a role of *miR-19s* in the IL-6 antiapoptotic signal in the pathogenesis and malignant growth of MM.

***miR-17∼92* Cluster Target BIM in MM Cells.** Because the *miR-17∼92* cluster has been shown to target the proapoptotic gene, BIM (19–20), we examined whether BIM expression is modulated by *miR-17∼92* in MM cells. U266 cells were transfected with *miR-19s* ASOs and BIM expression was evaluated using immunoblot. We found a significant increase of BIM protein levels at 48 h after treatment with anti-*miR-19s* compared to scrambled oligonucleotides (Fig. S5). Together, these results have supported previous published data (19–20) that show BIM as a direct target of *miR-17∼92* and suggest a possible mechanism through which over-expression of *miR-17∼92* contributes to the antiapoptotic signals in MM.

Ectopic Repression of *miR-19s* and *miR-181a* and *b* in MM Cell Lines Leads to Significant Suppression of Tumor Growth in Nude Mice. To explore the *in vivo* relevance of our observations, we examined the tumorigenicity of U266 and JJN3 cells in athymic *nu/nu* mice after silencing of the endogenous *miR-19s* and *miR-181a* and *b*. Two independent experiments, each using 16 mice for each cell line, were conducted. U266 or JJN3 cells were transfected with ASOs or scrambled oligonucleotides *in vitro*. We confirmed transfection efficiency (80% for U266 and JJN3) using BLOCK-IT Fluorescent Oligo (Invitrogen). Twenty-four hours later 3×10^7 viable cells for each group, re-suspended in 100 μl of BD matrigel matrix, were injected s.c. into the right flank of nude mice. The relative expression levels of the endogenous

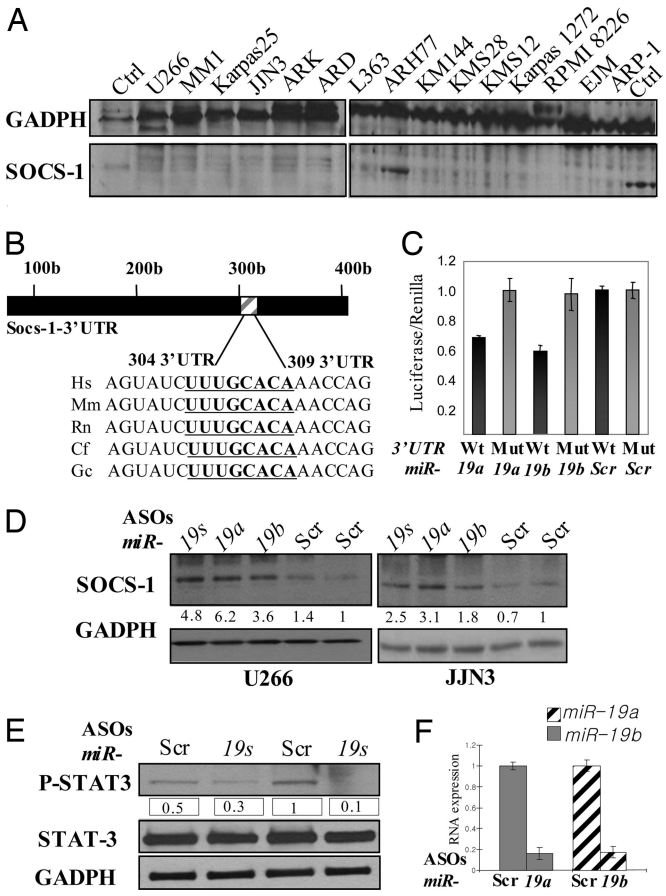

Fig. 3. *miR-19s* target SOCS-1 in MM cell lines. (*A*) Immunoblot analysis with antisera against SOCS-1 and GADPH in 15 MM cell lines and two CD138+PCs from healthy donors (control). (*B*) Predicted highly conserved consensus binding site in human, mouse, rat, and dog for *miR-19s* on the 3′UTR of SOCS-1. (*C*) Relative luciferase activity in MEG01 cells transiently cotransfected with luciferase reporter vector containing the 3′ UTR of *SOCS-1* and *miR-19s* or scrambled oligonucleotides. Deletion of the six bases in the putative *miR-19s* binding site, complementary to miRNA seed region, abrogates this effect (MUT). Bars indicate firefly luciferase activity normalized to Renilla luciferase activity ± SD. Each reporter plasmid was transfected at least twice (on different days) and each sample was assayed in triplicate. (*D*) Western blot showing SOCS-1 protein in whole cell lysates from U266 and JJN3 cells at 48 h after transfection with scrambled oligonucleotides or *miR-19a*, *miR-19b*, or both ASOs. GADPH was used as loading control. Densitometry based on GADPH levels shows increased level of SOCS-1 in presence of *miR-19a* or *miR-19b* or together ASOs in U266 and JJN3 cells. (*E*) Western blot showing that *miR-19s* modulate expression of activated STAT-3 in U266 cells *in vitro*. Cells were transfected with anti-*miR-19s* or negative control (Scr) miRNA inhibitors *in vitro*, and cell lysates were obtained after 72 h. Densitometry based on STAT-3 levels shows decreased level of P-STAT-3 in presence of *miR-19s*. (*F*) Stem-loop q-RT-PCR to validate the expression of endogenous *miR-19a* and *miR-19b*, at 72 h after transfection of U266 cells with antagonizing oligonucleotides, after normalization with RN*U6*B.

miR-19s and *miR-181a* and *b* after ASO transfection was assessed by q-RT-PCR to confirm the down-regulation of these miRNAs in both MM cell lines (data not shown). We found that after 2 weeks of cell inoculation, 70% of mice injected with MM cells transfected with scrambled oligonucleotide developed measurable tumors. By contrast, mice transplanted with cells expressing antagomiRs showed significant inhibition of tumor growth compared with controls ($P < 0.01$) (Fig. 4 *A* and *B*). Both cell lines treated with anti-*miR-19s* showed tumor volumes >10-fold reduced and tumors treated with antago *miR-181s* were three times smaller in JJN3 cells and 10 times smaller in U266 cells,

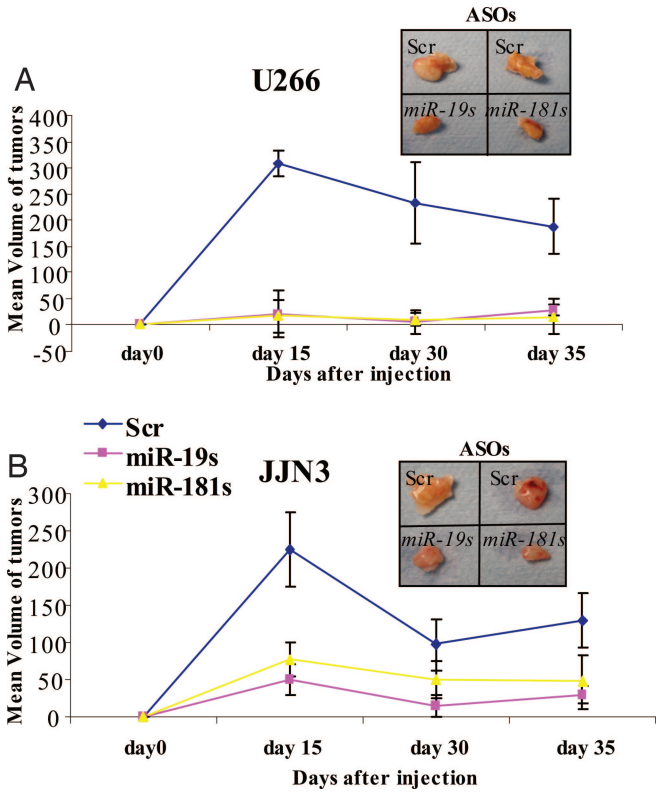

Fig. 4. Antagonizing *miR-19s* and *miR-181s* expression in MM cell lines resulted in significant tumor suppression in nude mice. U266 and JJN3 cells (30×10^6 cells) were injected subcutaneously into the flanks of nude mice with 100 μl of matrigel solution 24 h after transfection with *miR-19s* and *miR-181s* ASOs or scrambled oligonucleotide. Mice were killed on day 35 and tumor volumes were calculated. (*A*) Time course of tumor growth of U266 cell line. (*B*) Time course of tumor growth of JJN3 cell line; tumors treated with *miR-19s* and *miR-181s* ASOs were significantly smaller than tumors of scrambled groups for both cell lines. (Scale bar, 10 mm.)

$P = 0.02$ and $P = 0.01$, respectively. Importantly, complete tumor suppression was observed in two mice injected with U266 cells treated with anti-*miR-19s*. The average tumor volume after 4 weeks for U266 cells was 308.5 mm^3 and for JJN3 cells was 225 mm^3. Only 50% of mice injected with MM cells transfected with the antago *miR-19s* and *miR-181s* developed measurable tumors at 4 weeks. The average tumor volume for U266/anti-*miR-19*s was 19.5 mm^3 and for U266/anti-*miR-181s* was 14 mm^3. Similar results were observed with JJN3 MM cells, with average tumor volumes of 25 mm^3 and 80 mm^3 for anti-*miR-19s* and anti-*miR-181s*, respectively (see Fig. 4 *A* and *B*). Taken together, these results strongly suggested an oncogenic role of these miRNAs in MM and we speculate that the stronger effect of anti-*miR-19s* is related to the IL-6 dependence of U266.

Discussion

Over the past few years several studies have illustrated the biological relevance of miRNAs for the differentiation of normal hematopoietic cells and the contribution of deregulated miRNA expression in malignant counterparts (11, 30, 31). Our study has provided a unique comprehensive global miRNA expression profiling of MM, MGUS and contrasted these expression patterns with that of normal PCs. The similar miRNA expression pattern observed in MM cell lines and in primary newly diagnosed MMs supports the research design of this study. In addition, previous MM microarray studies have combined MM cell lines with primary patient samples, validating our strategy (32). We sought to identify a miRNA signature that could be associated with a MM multistep transformation process from normal PCs via MGUS to clinically overt myeloma, conscious of limitations because of the low number of MGUS and primary tumor samples. In MGUS patients, we identified up-regulated miRNAs with oncogenic function, such as the *miR-21* and the *miR-106b~25* cluster. *MiR-21* is up-regulated in many solid and hematological tumors (11, 25). The ectopic expression of *miR-21* in glioblastoma cells blocks apoptosis (33), while silencing its expression in several cancer cells inhibits cell growth and leads to increased apoptotic cell death by unblocking the expression of its targets: tumor suppressor genes like phosphatase and tensin homolog (*PTEN*) and protein programmed cell death 4 (*PDCD4*) (34). Petrocca and colleagues (20), have shown that the *miR-106b~25* cluster plays a role in gastric cancer tumorigenesis by targeting the proapoptotic BIM and p21. Thus, these two miRNAs may contribute to earlier steps in plasma cell transformation by blocking apoptosis, promoting PC survival, and predisposing to secondary genetic abnormalities that will ultimately result in a full blown malignancy.

In MM (including MM cell lines and primary tumors versus normal PCs) we identified a signature comprised of multiple up-regulated miRNAs, including among others *miR-32*, *miR-21*, *miR-17~92*, *miR-106~25*, and *miR-181a* and *b*. While *miR-106~25*, *miR-181a* and *b*, and *miR-21* were up-regulated also in MGUS patients with respect to normal PCs, *miR-32* and the *miR-17~92* cluster were highly expressed only in MM patients, suggesting that these miRNAs are MM-specific. Besides RAS mutations, no other genetic abnormality has been found to differentiate MGUS from MM (3). Therefore, *miR-32* and the *miR-17~92* cluster may represent MM-specific genetic changes. However, this will require further independent validation because we used a small number of patient samples and normal plasma cells.

Similar to the *miR-106~25* cluster, the oncogenic role of the *miR-17~92* cluster in B cell lymphoma is well known and several known proapoptotic genes, including *PTEN*, *E2F1*, and *Bcl2l11/BIM* are confirmed as targets of *miR-17~92* (35–36). Recently, Ventura and colleagues (19) have shown that the *miR-17~92* cluster is also essential for B cell development and that the absence of *miR-17~92* leads to increased levels of the proapoptotic protein BIM and inhibits B cell development at the pro-B to pre-B transition. However, given the nearly identical sequences, it is very likely that *miR-106b~25* and *miR-17~92* clusters cooperate in exerting similar, if not identical, functions as in targeting *BIM* (19–20).

Our study provided important functional insights about miRNAs deregulated in MM. We have confirmed that the proapoptotic BIM is a target of the *miR-17~92* cluster in MM cells. Therefore, *miR-17~92*, along with *miR-21*, blocks apoptosis and promotes cell survival. On the other hand, *miR-106b~25*, *miR-181a*, and *miR-32* but not *miR17~92* cluster (specifically *miR-19s* and *miR-92*), target PCAF, a p53 positive regulator. We speculate, consistent with the low frequency of p53 mutations in MM, that down-regulation of PCAF by the *miR-106b~25* cluster, *miR-181s*, and *miR-32*, keeps p53 at low level or partially inactivated by controlling its stability through Hdm2 (24) and working as a histone acetyltransferase (23). We have also described the specific role of *miR-19s* on the STAT-3/IL-6R negative regulator SOCS-1. In fact, IL-6 pathways in MM are among the best characterized survival pathways participating in PC transformation and oncogenesis through STAT-3, impacting apoptosis regulators such as the Bcl-2 family members (1, 16). Our findings demonstrate that the up-regulation of *miR-19s* in MM could contribute to SOCS-1 down-regulation and IL-6 activation at later stages in MM pathogenesis.

The role of *miR-19s* and *miR-181s* in MM cells as oncomiRNAs was confirmed by *in vivo* studies. Our data demonstrate

significant tumor regression of transplanted tumors after treatment with *miR-19s* and *181s* antagomiRs. These data may suggest that miRNAs could have a therapeutic potential in antagonizing the growth of transformed PCs.

In conclusion, we reported distinctive miRNA signatures in MM and MGUS, characterized by over-expression of miRNAs with known oncogenic activity. Our data provided insights into the miRNA function in MM by establishing links with the regulation of critical pathways in MM by miRNAs, including apoptosis, survival, and proliferation. These results indicate an additional level of control by this class of regulatory molecules in the multistep process associated with malignant transformation of PCs.

Materials and Methods

RNA Extraction and miRNA Microarray Experiments. RNA extraction and miRNA microchip experiments were performed as described in detail elsewhere (37). The miRNA microarray is based on a one-channel system (35). Five micrograms of total RNA was used for hybridization on the Ohio State University custom miRNA microarray chips (OSU_CCC version 3.0), which contains ≈1,100 miRNA probes, including 345 human and 249 mouse miRNA genes, spotted in duplicates.

RT-PCR. The single tube TaqMan miRNA assays were used to detect and quantify mature miRNAs as previously described (10) using ABI Prism 7900HT sequence detection systems (Applied Biosystems). Normalization was performed with RN*U6*B. Comparative real-time PCR was performed in triplicate, including no-template controls. Relative expression was calculated using the comparative C_t method.

ASOs and Mimics Transfection Experiments. Cells were transfected by using nucleoporation (Amaxa) kit V (for JJN3 and MM1s cell lines) and kit C (for U266 cell line) using 100 nM miRNA precursors (Ambion), or 100 nM LNA miRNA antisense oligonucleotides (Ambion). Protein lysates and total RNA were collected at the time indicated. miRNA processing and expression were verified by Northern blot and stem-loop q-RT-PCR. We confirmed transfection efficiency (≈80% for U266 and JJN3 and 50% for MM1s) using BLOCK-IT Fluorescent Oligo (Invitrogen) for all of the cell lines. Untreated cells transfected with negative control oligonucleotides were used as a calibrator.

ACKNOWLEDGMENTS. We thank Dr. Kay Huebner and Dr. Hiroshi Okumura for their support and scientific advice, Dorothee Wernicke-Jameson for research supervision, and Sharon Palko for administrative support. This work was supported by National Cancer Institute grants (to C.M.C.), Kimmel Foundation awards (to R.I.A., N.Z., and R.G.), and an Ohio Cancer Research Associates grant (to R.I.A.).

1. Bommert K, Bargou R, Stühmer T (2006) Signalling and survival pathways in multiple myeloma. *Eur J Cancer* 42:1574–1580.
2. Fonseca R, San Miguel J (2007) Prognostic factors and staging in multiple myeloma. *Hematol Oncol Clin N Am* 21:1115–1140.
3. Hideshima T, Mitsiades C, Tono G, Richardson PG, Anderson KC (2007) Understanding multiple myeloma pathogenesis in the bone marrow to identify new therapeutic targets. *Nat Rev Cancer* 7:585–598.
4. Oancea M, Mani A, Hussein MA, Almasan A (2004) Apoptosis of multiple myeloma. *Int J Hematol* 80:224–231.
5. Drach J, *et al.* (1995) Multiple myeloma: High incidence of chromosomal aneuploidy as detected by interphase fluorescence in situ hybridization. *Cancer Res* 55:3854–3859.
6. Latreille J, Barlogie B, Johnston D, Drewinko B, Alexanian R (1982) Ploidy and proliferative characteristics in monoclonal gammopathies. *Blood* 59:43–51.
7. Chng WJ, Glebov O, Bergsagel PL, Kuehl WM (2007) Genetic events in the pathogenesis of multiple myeloma. *Best Pract Res Clin Haematol* 20:571–596.
8. Calin GA, *et al.* (2005) A microRNA signature associated with prognosis and progression in chronic lymphocytic leukemia. *N Engl J Med* 353:1793–1801.
9. Garzon R, *et al.* (2008) MicroRNA signatures associated with cytogenetics and prognosis in acute myeloid leukemia. *Blood* 111:3183–3189.
10. Bartel D (2004) MicroRNAs: Genomics, biogenesis, mechanism, and function. *Cell* 116:281–297.
11. Croce CM (2008) Oncogenes and cancer. *N Engl J Med* 358:502–511.
12. Garzon R, *et al.* (2007) MicroRNA gene expression during retinoic acid-induced differentiation of human acute promyelocytic leukemia. *Oncogene* 26:4148–4157.
13. Calin GA, Croce CM (2006) MicroRNA signatures in human cancers. *Nat Rev Cancer* 6:857–866.
14. Löffler D, *et al.* (2007) Interleukin-6 dependent survival of multiple myeloma cells involves the Stat3-mediated induction of microRNA-21 through a highly conserved enhancer. *Blood* 110:1330–1333.
15. Seidl S, Kaufmann H, Drach J (2003) New insights into the pathophysiology of multiple myeloma. *Lancet Oncol* 4:557–564.
16. Chen CZ, Li L, Lodish HF, Bartel DP (2004) MicroRNAs modulate hematopoietic lineage differentiation. *Science* 303:83–86.
17. Liu CG, Calin GA, Volinia S, Croce CM (2008) MicroRNA expression profiling using microarrays. *Nat Protoc* 3:563–578.
18. He L, *et al.* (2005) A microRNA polycistron as a potential human oncogene. *Nature* 435:828–833.
19. Ventura A, *et al.* (2008) Targeted deletion reveals essential and overlapping functions of the miR-17 through 92 families of miRNA clusters. *Cell* 132:875–886.
20. Petrocca F, *et al.* (2008) E2F1-regulated microRNAs impair TGFbeta-dependent cell-cycle arrest and apoptosis in gastric cancer. *Cancer Cell* 13:272–286.
21. Lewis B, Shih I, Jones-Rhoades M, Bartel D, Burge C (2003) Prediction of mammalian microRNA targets. *Cell* 115:787–798.
22. Krek A, *et al.* (2005) Combinatorial microRNA target prediction. *Nat Genet* 37:495–500.
23. Schiltz RL, Nakatani Y (2000) The PCAF acetylase complex as a potential tumor suppressor. *Biochim Biophys Acta* 1470:M37–M53.
24. Linares LK, *et al.* (2007) Intrinsic ubiquitination activity of PCAF controls the stability of the oncoprotein Hdm2. *Nat Cell Biol* 9:331–338.
25. Imamura J, Miyoshi I, Koeffler HP (1994) p53 in hematologic malignancies. *Blood* 84:2412–2421.
26. Stühmer T, Bargou RC (2005) Selective pharmacologic activation of the p53-dependent pathway as a therapeutic strategy for hematologic malignancies. *Cell Cycle* 5:39–42.
27. Greenhalgh CJ, Hilton DJ (2001) Negative regulation of cytokine signaling. *J Leukoc Biol* 70:348–356.
28. Galm O, Yoshikawa H, Esteller M, Osieka R, Herman JG (2002) SOCS-1, a negative regulator of cytokine signaling, is frequently silenced by methylation in multiple myeloma. *Blood* 101:2784–2788.
29. Schwab G, Siegall CB, Aarden LA, Neckers LM, Nordan RP (1991) Characterization of an interleukin-6-mediated autocrine growth loop in the human multiple myeloma cell line, U266. *Blood* 77:587–593.
30. Volinia S, *et al.* (2006) A microRNA expression signature of human solid tumors defines cancer gene targets. *Proc Natl Acad Sci USA* 103:2257–2261.
31. Garzon R, *et al.* (2008) Distinctive microRNA signature of acute myeloid leukemia bearing cytoplasmic mutated nucleophosmin. *Proc Natl Acad Sci USA* 105:3945–3950.
32. Zhan F, *et al.* (2002) Global gene expression profiling of multiple myeloma, monoclonal gammopathy of undetermined significance, and normal bone marrow plasma cells. *Blood*, 99:1745–1757.
33. Chan JA, Krichevsky AM, Kosik KS (2005) MicroRNA-21 is an antiapoptotic factor in human glioblastoma cells. *Cancer Res* 65:6029–6033.
34. Meng F, *et al.* (2007) MicroRNA-21 regulates expression of the *PTEN* tumor suppressor gene in human hepatocellular cancer. *Gastroenterology* 133:647–658.
35. Novotny GW, *et al.* (2007) Translational repression of E2F1 mRNA in carcinoma *in situ* and normal testis correlates with expression of the miR-17–92 cluster. *Cell Death Differ* 14:879–882.
36. O'Donnell KA, Wentzel EA, Zeller KI, Dang CV, Mendell JT (2005) c-Myc-regulated microRNAs modulate E2F1 expression. *Nature* 435:839–843.
37. Liu CG, *et al.* (2004) An oligonucleotide microchip for genomic-wide microRNA profiling in human and mouse tissues. *Proc Natl Acad Sci USA* 101:9740–9744.